

# Structure and Properties of Coatings on Ni Base Deposited using Plasma Jet Before and After Electron Beam Irradiation

A.D. Pogrebnyak<sup>1,4</sup>, V.V. Vasyliuk<sup>1</sup>, Sh.M. Ruzimov<sup>2</sup>,  
V.V. Ponaryadov<sup>3</sup>, S. Kuroda<sup>6</sup>, K. Dyadyura<sup>1</sup>, S.N. Kislitsyn<sup>6</sup>

1. Sumy Institute for Surface Modification, P.O.Box 163, St. Romenskaya 87, Bld. "M", 40030 Sumy, Ukraine

2. National University of Uzbekistan, Tashkent, Uzbekistan

3. Belarus State University, Minsk, Belarus

4. Department Surface Beam Modification, Institute for Metal Physics, NAs of Ukraine, St. Romenskaya 87, Bld. "M", 40030 Sumy, Ukraine

5. National Institute of Materials Research Tsukuba, Ibaraki, Japan.

6. Nuclear Physics Institute, NNC Almaty, Kazakstan

**Abstract** – Experimental results for structure, morphology, phase composition and measurements of nano- and microhardness, wear resistance, and adhesion of coatings on Ni base, which were deposited using a plasma jet, before and after pulsed plasma jet and high-current electron beam melting are presented. Newly formed phases like Cr<sub>3</sub>Ni<sub>2</sub> and CrB and intermetallic compounds with molybdenum like Fe<sub>7</sub>Mo<sub>6</sub>, Fe<sub>3</sub>Mo and possibly Fe Mo were found. We also found an effect of phase composition, changed grain dimension and smoothed relief resulting in a factor of three increase in micro- and nanohardness, almost a factor of 20 increase in friction wear resistance and several times increase in coating to substrate adhesion.

## 1. Introduction

The goal of this work was to study morphological features of Ni-based powder coatings surfaces, to determine phase and element composition and mechanical characteristics (nano- and microhardness, friction wear, adhesion and corrosion resistance in seawater) resulting from various treatment conditions.

## 2. Materials and Investigation Methods

PGAN-33 powder (Ni – the base; Cr – 22 to 24 %; Mo – about 4 %; Si – about 2 %; W – about 1 to 1.5 %; B – about 2 %, Russia standard) was used as initial material for producing wear and corrosion resistant experimental coatings. By introducing Mo and W into the powder initial material and simultaneously applying an eroding molybdenum electrode, we increased a resulting coating hardness. Dimensions of steel3 (Fe – the base; C – about 0.14 to 0.22 %; Mn – about 0.4 to 0.65 %; Si ≤ 0.15 %) samples were 50×50×3.2 mm<sup>3</sup>. The samples were preliminarily subjected to jet-abrasive treatment. Electro-corundum was used as an abrasive material. Then a coating of 120 to 150 μm thickness were deposited to these samples using a high-velocity plasma jet.

Coating on nickel base were deposited to the steel 3 substrate using a facility "Impulse-5", which operation regimes were the following: capacity of a conden-

ser battery – 800 μF; impulse repetition frequency – 3 Hz; plasma jet velocity – 7.5 to 7.8 km/sec; plasma flow temperature – 3·10<sup>4</sup> K; total amount of combustion mixture components – 2 m<sup>3</sup> per hour; a distance from the plasmatron nozzle to the substrate – 0.04 m. Taking into account melting temperature of nickel-based powder, we selected parameters of a pulsed-plasma flow allowing us for one impulse ( $t \approx 4 \cdot 10^{-3}$  s) to melt totally the coating and partially the substrate. Powder expenditures were about 225 g/min. Repetition frequency of impulses was  $\nu = 4$  Hz. The condenser battery capacity of a discharge contour was  $C = 800 \mu\text{F}$ , voltage at the condenser covers being  $U = 3$  kV. Propane expenditures in a combustion chamber was  $G_{\text{Cr}} = 0.16$  m<sup>3</sup>/hour. Oxygen expenditures in the combustion chamber was  $G_{\text{O}_2} = 1.18$  m<sup>3</sup>/hour.

Surface melting of plasma-detonation coatings was realized using a source U-212 with 30 kV energy by beam scanning over the sample surface with a path width reaching 12 mm. Power density of the electron beam was  $(1 \text{ to } 2) \cdot 10^3$  W/cm<sup>2</sup>, motion of an electron beam over the substrate surface was 1.5 m/s, and the treated pass width was  $(10 \text{ to } 12) \cdot 10^{-2}$  m.

This work presents results of studies for four series of samples: series N1 presented a sample with an initial coating; series N2 presented a sample with a pulsed-plasma melted powder coating and a partially melted substrate surface (melting depth was about  $4 \cdot 10^{-3}$  m); series N3 presented a sample with a totally melted by an electron beam coating and a substrate melted to 1.5 to  $2 \cdot 10^4$  m depth; series N4 presented a sample with a totally melted coating and a substrate melted to  $1.5 \cdot 10^{-4}$  m, then about 30 μm was taken away using an abrasive disc with subsequent diamond paste polishing.

Studies of the surface structure were performed using a scanning electron microscope REMMA-102 (Selmi, Sumy, Ukraine) with a micro-analyzer (EDS) and (WSD). Surface phase composition was determined using X-ray diffraction facility RDON-2 (St. Petersburg, Russia) in CuK<sub>α</sub> emission. Interpretation of

diffraction patterns peaks was performed using reference books [7] and a license data base PCPDFWIN (80000 compounds). Simultaneously studies of surface phase composition were performed using a method of low-angle scattering of a X-ray diffraction facility D8 Advance (Bruker AXS, Germany, 2000) in  $\text{CuK}_\alpha$  emission. Decoding and interpretation of diffraction patterns was performed using a license data base containing the data about more than 140000 compounds and a set of programs for data processing Diffrac Plus.

1. Measurements of micro-hardness were performed both over the surface and across transversal and angular cross-sections using a facility PMT-3 (St. Petersburg, Russia), an indentation load being 2; 5; 10 N. Also using a three face Berkovitch indenter Nano Indenter-II, MTS Systems Corporation, Oak Ridge, TN, USA, we measured nano-hardness. A measurement accuracy of indentation depth was  $\pm 0.04$  nm, an indentation load being  $\pm 75$  nN.

Rate of loading rise was 0.5 nN/sec.

Tests of wear resistance were performed using SMTS-2 facility (Ukraine) according to a scheme "plane-cylinder" in a technical Vaseline environment (a load was 10 N). Bulk mass ablation was measured every 500 cycles (turnings of a counter-body). Total number of turnings was 10000. Length and width of a worn area induced by a touching counter-body with a tested sample was measured versus the number of the counter-body turnings N.

### 3. Experimental Results and Discussion

Plasma-detonation deposition of powder coatings is accompanied by formation of a silver-gray layer of 150 to 160  $\mu\text{m}$  thickness on a stainless steel substrate. According to the known papers, coating deposition [7] comprises two characteristic stages, as a result of which atoms of various substances form bindings both in the powder and in the contact region of the coating and substrate. Additionally some fraction of an initial material may form strong compounds or substitution solid solutions due to chemical interaction of their components. After depositing coatings the samples were treated by an electron beam till total melting of the coating and partial melting of the substrate to 120–150  $\mu\text{m}$  depth and till total melting of the coating and little melting of the substrate surface layer. Fig. 1, *a*, *b* demonstrates volume fractions of the phases found in the coating surface layer for the two applied regimes. One can note that in addition to changing per cent phase ratio one can find also newly formed phases. For example, in the case of lower energy density in the coating one can find 50 %Ni; 20 %Mo; 15 %FeMo+Fe<sub>7</sub>Mo<sub>6</sub>; about 15 %FeCr. Having increased the energy density, one can find in the coating about 40 %Ni; about 20 %Cr<sub>3</sub>Ni<sub>2</sub> (this compound is absent in the above mentioned coating) and 40 %FeMo-Fe<sub>7</sub>Mo<sub>6</sub>+Mo. Surface melting by concentrated energy flows provides total or partial pores and defects sealing in an already formed surface structure and formation of new compounds in the process of surface structure melting [5, 6, 9 and 10] (See further the results of SEM analysis).

Evaluation of Ni lattice parameters indicates a number of essential changes in the initial powder content. It seems to be due to tensile stress, which results from formation of a substitution solid solution of nickel atoms by coating composing elements (evidently chromium atoms) inducing finally an increase in the lattice parameter:  $a(\text{Ni})=3.53$  Å ( $a_{\text{table}}(\text{Ni})=3.52$  Å [7]).

Figure 3 shows a diffraction pattern taken for a coating irradiated by higher density electron beam, after removing a layer of not less than 30 $\mu\text{m}$  from this coating. Interpretation of X-ray patterns demonstrated that two basic phases were present in the coating: a cubic face-centered one with a crystal lattice period  $a=3.587$  Å and a cubic bulk-centered one with a period  $a=2.869$  Å. Taking into account the element composition of the sample and values of lattice periods, the face-centered cubic phase was related to Fe<sub>0.64</sub>Ni<sub>0.36</sub>, which standard X-ray data were taken from PDF-2 N47-1405. The bulk-centered cubic phase was related to a solid solution on iron base, since a calculated period of this phase was  $a=2.869$  Å, which a little higher than for a pure iron ( $a=2.866$  Å). A third phase was found in this sample, which was identified as Fe<sub>2</sub>B and little in amount. The X-ray pattern also shows a weak in intensity line 2.387 Å, which can be related to Fe<sub>3</sub>C cementite.

The data show a total spectrum of phases formed in this coating: Ni<sub>6</sub>Cr<sub>6</sub>Si<sub>7</sub>; Fe<sub>0.64</sub>Ni<sub>0.36</sub>; FeN<sub>3</sub>; Ni<sub>3</sub>B; Ni<sub>16</sub>, ratio of which can hardly be counted since many phases overlap. Upon treating the coating by a plasma jet till melting, such phases as FeNi<sub>3</sub>; NiFe<sub>2</sub>O<sub>4</sub> and Ni<sub>3</sub>B were formed in the surface layer.

Electron-microscopy studies of the coatings surfaces after duplex modification revealed the following features of the powder layer structure. Plasma-detonation deposition of the coatings was accompanied by formation of a surface layer with high roughness. Pulsed-plasma melting (series N2) resulted only in partial decrease of the roughness. Fig. 4, *a* shows a general view of coating surface. As one can see, a produced structure comprises many hills smoothly developing into valleys. 1000 to 2000 times magnification allowed us to find frozen slightly deformed powder particles (Fig. 4, *b*, the particle is marked by +). We assume that in the process of plasma-detonation deposition these particles reach the base in partially melted state. Due to Van der Waals forces and mechanical and chemical actions totally melted powder particles are glued to the melted base surface, and partially melted particles are sealed into a detection layer (their distribution seems to be chaotic over the total coating surface). Pulsed-plasma surface melting resulted only in partial valleys sealing. Surface photographs of 300 to 600 times magnification demonstrate many smooth dark regions with a pronounced grain structure and many valleys with a sharp relief bottom. And namely in the vicinity of these valleys we observed regions with the morphology, which was similar to melted deformed powder particles.

As one can see, roughness decreased over all irradiated part of the sample. However, there are regions

with very high roughness, which was formed as a result of melting. There are also regions with not fully melted powder particles – it seems that these regions comprise refractory elements and their carbides (results of microanalysis). Analysis of the coating cross-section structure after duplex treatment demonstrated that depending on electron beam energy density an average grain dimension within the depth from the surface vicinity to 9–15  $\mu\text{m}$  decreased from hundreds of micrometers to units of a micron and hundreds of nanometers.

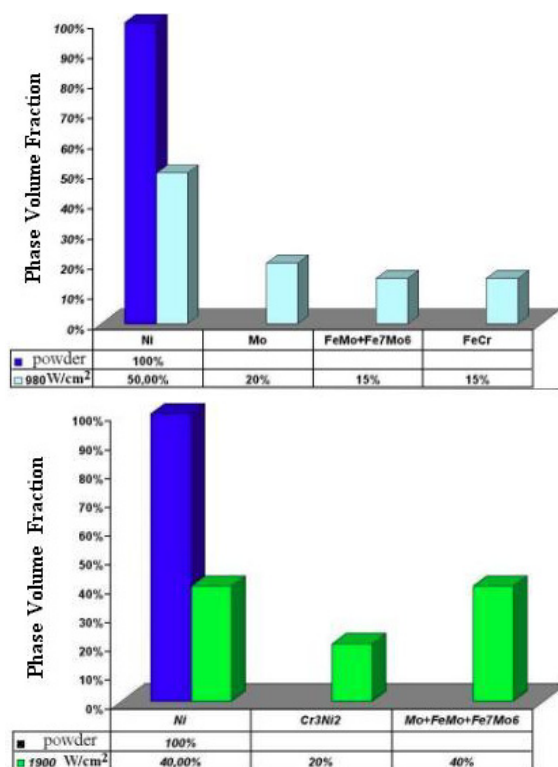


Fig. 1. Histograms of a per cent phase ratio obtained from the diffracts of a patterns (Fig. 1, a, b) for PGAN-33 coatings: a – treatment conditions (see Fig. 1, a); b – treatment conditions (see Fig. 1, b)

The image shows a typical surface morphology – "an orange peel" [1, 6, 11]. Two regions show hills of big dimensions – 6 to 8  $\mu\text{m}$ , an average roughness range being 1.5 to 2  $\mu\text{m}$ . We performed a local analysis in the biggest hill. The resulting spectrum shows that the base of this hill comprises 64 %Ni; more than 17 %Fe; about 13 %Cr and about 4.8 %Cr. Local microanalysis taken from the surface regions after duplex treatment (in light zones) demonstrated that in these surface parts there are about 70 %Mo, about 20 %Ni; about 4 %Si; about 3.5 %Cr and 2 %Fe. Mo appeared in the process of surface treatment by high-velocity plasma jet from an evaporated eroding electrode.

Figure 3, a and b shows loading curves for the samples melted by an electron beam (full melting, about 2 kW/cm<sup>2</sup>). Maximum nanohardness was lower a little than 6.1 GPa. Another series of samples, where the coating was melted by high-velocity plasma jet, acquired maximum value of nanohardness 6.8 GPa,

and a transition (interface) layer between the coating and substrate and 3.9 to 3.7 GPa  $\pm 0.5$ , real substrate nanohardness being about 1.78  $\pm 0.03$  GPa.

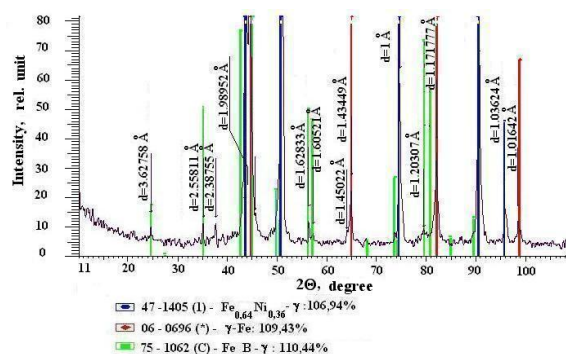


Fig. 2. Diffraction patterns (XRD) for steel sampled with PGAN-33 coatings of about 120  $\mu\text{m}$  which were deposited using high-velocity plasma jet with subsequent melting by an electron beam of 2 kW/cm<sup>2</sup> power density. Then a layer of about 30  $\mu\text{m}$  thickness was put away from the resulting coating using abrasive method and finally polished by diamond paste with grain dimensions 9, 5 and 2  $\mu\text{m}$

These results show that maximum hardness of coatings deposited by a high-velocity pulsed plasma jet and melted by an electron beam was found in the surface and in the near surface region of the coating. Its values reached 320  $\pm 30$  kg/mm<sup>2</sup>. The increase in microhardness seems to be explained by formation of solid compounds of iron with molybdenum in the coating.

Deeper in the coating surface material microhardness decreased to 150  $\pm 30$  kg/mm<sup>2</sup>. Enrichment of the substrate surface by nickel powder comprising elements and those from plasmatron gas atmosphere, as well as its high-velocity electron quenching provide microhardness increase to 210  $\pm 30$  kg/mm<sup>2</sup> in comparison with the data for substrate initial state (Hmean of 140  $\pm 30$  to 160  $\pm 30$  kg/mm<sup>2</sup>). Increased substrate hardness induced by electron beam melting of deposited coatings was found at 300 to 400  $\mu\text{m}$  depth from the coating surface. Its value in this region was within the range of 190  $\pm 30$  to 210  $\pm 30$  kg/mm<sup>2</sup>.

At the same time highest microhardness of 700  $\pm 30$  kg/mm<sup>2</sup> was found in a coating after plasma-detonation deposition (without melting). Nanohardness also had high value of 6.8 GPa after plasma jet melting and a little lower one in the case of electron beam irradiation under 1 kW/cm<sup>2</sup>.

Most probable is that such increase in microhardness was conditioned by a phase composition of resulting coatings. In particular, after pulsed plasma melting in a coating surface we found the elements comprising the following materials: molybdenum, nickel, and intermetallic compounds of iron with molybdenum. In the region of a transition zone coating-substrate we found an impetuous decrease in material microhardness – to 300  $\pm 30$  kg/mm<sup>2</sup>. Due to thermal surface quenching the substrate had microhardness which was two times higher than that found at the boundary of an electron melting zone.

Figures 8a and 8b show that substrate microhardness depth dependence has a wavy character. Selected regimes of modification resulted in layer-by-layer hardening of the substrate passing gradually to the rare target side. In our case we observed substrate hardening occurring out of the zone of concentrated energy flow action. Deformation processes occurring out of the thermal action zone were induced by thermal-elastic wave, which was formed in the zone of energy absorption and then moved to the rare substrate side.

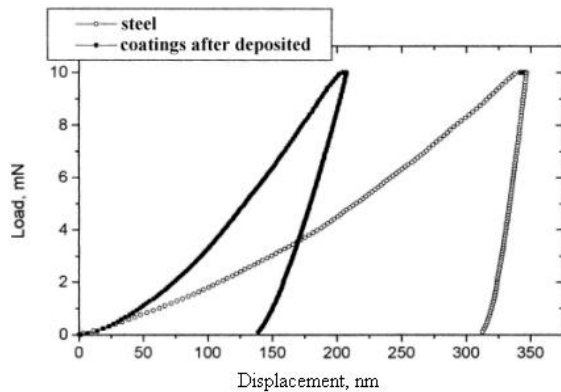


Fig. 3. Loading and unloading curves obtained using a nano-indenter for the coating which was deposited using high-velocity plasma jet and subsequent electron beam melting (results of analysis are shown in Table 3): a – after plasma jet melting with a melted layer thickness 45–50  $\mu\text{m}$ ; b – after electron beam melting under 2  $\text{kW}/\text{cm}^2$

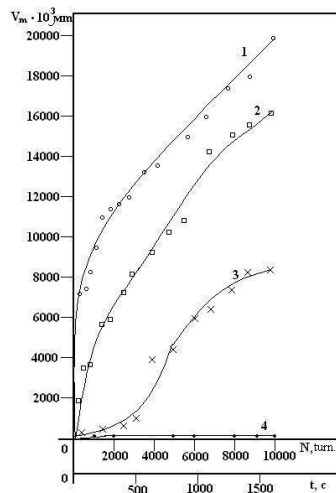


Fig. 4. Material friction ablation dependences (in technical Vaseline) on a number of revolutions and evaporation time: 1 – the curve for steel3 substrate; 2 – a curve for PGAN-33 coating on Ni base which was deposited by a high-velocity plasma jet; 3 – a curve for coating after subsequent plasma jet melting; 4 – a curve for coating after subsequent electron beam melting under 2  $\text{kW}/\text{cm}^2$  power density

Fig. 4 shows results of mechanical tests for friction and wear in plasma detonation produced coatings. Analysis of experimental data demonstrated that plasma-detonation deposition of PGAN-33 powder coating with subsequent electron beam melting was accompanied by a twenty-fold increase of wear resistance of the material. We assume that this result was due to pure iron enrichment of the coating surface and substrate in the process of their melting as well as formation of nickel and chromium plastic compounds with boron. Pulsed plasma flow melting resulted only in partial increase in material plasticity. In the process of our experiment we established that pulsed-plasma melting of nickel-based coatings provided two-fold increase in material wear resistance. Adhesion tests (scrubbing by a diamond pyramid) demonstrate that after PGAN-33 powder coating deposition adhesion was  $57 \pm 2$  MPa, after plasma jet action its average value increased non-essentially –  $61 \pm 2.5$  MPa. Melting of the coating by an electron beam of 1  $\text{kW}/\text{cm}^2$  energy essentially increased adhesion to  $144 \pm 3$  MPa, and electron beam irradiation of higher energy density – 2  $\text{kW}/\text{cm}^2$  – resulted in maximum value  $192 \pm 6$  MPa.

#### 4. Conclusions

Coating deposition by high-velocity plasma jet and subsequent treatment of the resulting coating by electron beam or a plasma jet allow one to form coatings with high mechanical characteristics. In both cases when coating surface structure was melted Ni lattice parameter was found to increase (with possible formation of substitution solid solution  $\text{Ni}_2\text{Cr}$ ). Electron beam and plasma induced melting of the coating surface was accompanied by its enrichment with a basic element of the substrate matrix ( $\alpha\text{-Fe}$ ) due to convection motion of liquid phase metal. It was established that plasma detonation induced surface melting of coatings by concentrated energy flows was accompanied by formation of solid intermetallic iron compounds with molybdenum ( $\text{Fe}_7\text{Mo}_6$ ,  $\text{Fe}_3\text{Mo}$ , and possibly,  $\text{Fe Mo}$ ). Due to high-temperature electron melting plastic intermetallic compounds  $\text{Cr}_3\text{Ni}_2$  and  $\text{CrB}$  are formed in the coating surface.

It induces:

1. increased microhardness of a surface layer in comparison with substrate, approximately, by a factor of 5 for the coatings melted by pulsed plasma flows, and a factor of 3 for coatings after electron beam modification;
2. a factor of 2 increase in coatings wear resistance after pulsed-plasma melting and a factor of 20 increase after electron beam melting;
3. a factor of 2 increase in coating nanohardness after repeated plasma jet treatment and several times increase in coating to substrate adhesion.

**References**

- [1] A.D. Pogrebnjak, Yu.N. Tyurin. *Uspekhi Fiziki Metallov* 4/1, 1 (2003).
- [2] Yu.N. Tyurin, A.D. Pogrebnjak. *Surf. and Coat. Tech.* 122, 269 (1999).
- [3] Yu.S. Borisov, Yu.N. Tyurin. *Hardening Treatment of Tools by High-Energy Plasma (rus)*. Preprint. O.E.Paton Electric Welding Institute. ISE-92 I.-K. 1992. 37 P.
- [4] V.A. Klimeonov, V.E. Panin, V.P. Bezborodov, O.B. Perevalova, Zh.G. Senchilo, E.V. Kozlov, V.G. Durakov. *Fiz. Khim. Obrabotki Materialov*. 6, 68 (1997).
- [5] O.P. Kul'ment'eva, A.D. Pogrebnjak, V.S. Kshnyakin, Yu.A. Skiba. *Fiz. Khim. Tverdogo Tela.* 3/1, 154 (2002).
- [6] A.A. Shipko, I.L. Pobol, I.G. Urban. *Hardening of Steels and Alloys Using Electron Beam Heating (rus)*. Monography. Nauka I Technika. 1995. V. 280. ISBN 5-343-00937-9.
- [7] S.S. Gorelik, L.N. Rastorguev, Yu.A. Skakov. *X-Ray and Electron Optical Analysis. Appendixes*. Moscow. Metallurgy. 1970. 108P.